PHYSICAL REVIEW D, VOLUME 64, 043502

Inelastic dark matter

David Smith
Department of Physics, University of California, Berkeley, California 94720
and Theoretical Physics Group, Ernest Orlando Lawrence Berkeley National Laboratory, University of California, Berkeley, California 94720

Neal Weiner
Department of Physics, University of Washington, Seattle, Washington 98195
(Received 15 February 2001; published 12 July 2001)

Many observations suggest that much of the matter of the universe is nonbaryonic. Recently, the DAMA NaI dark matter direct detection experiment reported an annual modulation in their event rate consistent with a WIMP relic. However, the Cryogenic Dark Matter Search (CDMS) Ge experiment excludes most of the region preferred by DAMA. We demonstrate that if the dark matter can only scatter by making a transition to a slightly heavier state ($\Delta m \sim 100$ keV), the experiments are no longer in conflict. Moreover, differences in the energy spectrum of nuclear recoil events could distinguish such a scenario from the standard WIMP scenario. Finally, we discuss the sneutrino as a candidate for inelastic dark matter in supersymmetric theories.

DOI: 10.1103/PhysRevD.64.043502 PACS number(s): 95.35.+d

I. INTRODUCTION

A central task of modern cosmology is to determine what the universe is made of. A number of observations suggest that the bulk of the matter in the universe is not luminous [1]. Direct searches for baryonic matter in the form of massive compact halo objects (MACHOs) cannot account for the matter that seems necessary to explain these observations [2].

An alternative explanation is that weakly interacting massive particles (WIMPs) exist copiously in the halo of our galaxy but only rarely interact with ordinary matter [3]. Candidate WIMPs from particle theory include the axion and the lightest supersymmetric particle (LSP) in supersymmetric theories with *R*-parity conservation.

Numerous experiments have been set up in attempts to directly detect WIMPs [4–6]. The two which are sensitive to the smallest spin independent cross sections are the Cryogenic Dark Matter Search (CDMS) Ge experiment [5] and the DAMA NaI experiment [6]. Recently, DAMA reported the presence of a signal consistent with a WIMP at better than 4σ. When interpreted as a standard WIMP with spin independent interactions, CDMS rules out nearly all of the DAMA 3σ preferred region at 90% confidence levels and all of it at 84% confidence levels. Attempts to reconcile these experiments using spin dependent interactions have been shown to be in gross conflict with indirect detection experiments and previous direct searches [7].

In this paper, we will show that a simple modification to the properties of the dark matter particle can change the kinematics of the scattering sufficiently to reconcile the two experiments. In particular, we explore the possibility of inelastic dark matter: relic particles that cannot scatter elastically off of nuclei. The outline of the paper is as follows: we begin by comparing the details of the two experiments and give a naive argument as to why inelastic dark matter can reconcile them. In Sec. II we explicitly calculate the event rate at CDMS and DAMA taking into account the inelasticity of the scattering. In Sec. III we use this calculation to study what differences can arise relative to the elastic case and to examine whether there are regions of parameter space that give a signal at DAMA but a null result at CDMS. In Sec. IV we discuss how inelastic dark matter could arise from a massive complex scalar split into two approximately degenerate real scalars, or from a Dirac fermion split into two approximately degenerate Majorana fermions. We also present a specific model, featuring a real component of the sneutrino as the dark matter, in which the mass splitting required to reconcile DAMA and CDMS arises naturally. In Sec. V we discuss direct detection possibilities at future experiments.

A. CDMS and DAMA

If we are to understand the DAMA signal as evidence of dark matter, but simultaneously accept the null result of CDMS, we must reconsider some basic element of the WIMP hypothesis. Before we address such a modification, we should understand the differences between the DAMA and CDMS experiments.

The DAMA experiment utilizes a set of NaI crystals at the Gran Sasso National Laboratory of INFN to search for WIMPs. The basic premise of the experiment is that if WIMPs are present in the galaxy, as the galaxy rotates we feel a ''wind'' of WIMPs which will scatter elastically off of the target nuclei. As the Earth moves in its orbit about the Sun, the flux and velocity distribution (as seen by a terrestrial observer) vary. Rather than attempt to directly discriminate signal events against background, the DAMA experiment seeks to measure this modulation. There are two basic controls to this experiment. First, the signal phase must coincide with the Earth's motion in the solar system, which moves maximally with the galactic rotation on June 2, and maximally against on December 2. The second requirement is that the signal must lie dominantly in the lowest energy bins—a characteristic signal of WIMP scattering.

In contrast, CDMS uses a smaller Ge target, but has excellent background rejection capable of distinguishing nuclear recoils from electron scatterings for scattering energies greater than 10 keV. As a consequence their limits are comparable to those that would have been expected from a null DAMA result.

Exclusion plots are typically given in the m_χ-σ_n plane, where m_χ is the mass of the candidate and σ_n is the scattering cross section per nucleon. Implicit is the assumption that there are no great modifications in the scattering process between the two experiments.

However, if the dark matter cannot scatter elastically, then kinematical effects substantially distinguish the experiments. Consider two states, χ_- and χ_+, with χ_+ only slightly heavier than χ_-, such that χ_- can only scatter by transitioning to χ_+. It is a simple kinematical constraint that χ_- can only scatter inelastically off of a nucleus with mass m_N if

$$\delta < \frac{\beta^2 m_\chi m_N}{2(m_\chi + m_N)}, \tag{1}$$

where δ is the mass splitting between χ_- and χ_+. The possibility of evading direct detection by having a large enough splitting δ was pointed out in [8]. Here we focus on the fact that the constraint of Eq. (1) becomes increasingly severe as m_N is decreased. Since iodine has an atomic number of 127, while germanium has an atomic number of 73, we have the prospect of a situation where particles will scatter at DAMA but not at CDMS. For $\beta c \approx 220$ km/s (a typical dark matter particle velocity), and $m_\chi = 100$ GeV, the limits are 11 keV for CDMS and 15 keV for DAMA. If the mass splitting δ were 13 keV, such a particle would be visible to DAMA but not CDMS.

Of course, in the halo of the galaxy there is a distribution of velocities, so the calculation is not as simple as we have just illustrated. In the full calculation, we will find that the values of δ relevant for reconciling the experiments are somewhat larger than 15 keV, and that the window for δ has a size $\sim$50–100 keV rather than $\sim$5 keV.

II. DIRECT DETECTION RATES

In this section we review the standard calculation of event rates at direct detection experiments [9]. The differential rate per unit detector mass is given by

$$\frac{dR}{dE_R} = N_T \frac{\rho_\chi}{m_\chi} \int_{v_{min}} dv\, v f(v) \frac{d\sigma}{dE_R}. \tag{2}$$

Here E_R is the recoil energy of the target nucleus, N_T is the number of target nuclei per unit mass, ρ_χ is the local density of dark matter particles of mass m_χ, $d\sigma/dE_R$ is the differential cross section for relic-nucleus scattering, and v and $f(v)$ are the relic speed and speed distribution function in the detector rest frame. We take $\rho_\chi = 0.3$ GeV/cm^3.

Because we are interested in spin-independent scattering, the differential cross section may be written

$$\frac{d\sigma}{dE_R} = \frac{m_N}{2v^2} \frac{\sigma_n}{\mu_n^2} \frac{(f_p Z + f_n(A-Z))^2}{f_n^2} F^2(E_R), \tag{3}$$

where m_N is the nucleus mass, μ_n is the reduced mass of the relic-nucleon system, f_n and f_p are the relative coupling strengths to neutrons and protons, and σ_n is the relic-neutron cross section at zero momentum transfer, in the elastic ($\delta = 0$) limit. We use the Helm form factor [10]

$$F^2(E_r) = \left(\frac{3 j_1(q r_0)}{q r_0}\right)^2 e^{-s^2 q^2}, \tag{4}$$

with $q = \sqrt{2 m_N E_R}$, $s = 1$ fm, $r_0 = \sqrt{r^2 - 5s^2}$, and $r = 1.2A^3$.

We assume a standard Maxwell-Boltzmann distribution for the relic velocities in the galactic rest frame, with a root-mean-squared velocity $v_{rms} = \sqrt{\tfrac{3}{2}} v_0$, where we take $v_0 = 220$ km/s to be the rotational speed of the local standard of rest (LSR). In our calculation we take the escape velocity to infinity for simplicity, when one really should take $v_{esc} \simeq 650$ km/s. By doing so we overestimate the signal for large values of the mass splitting δ. For a 100 GeV relic, this is a 10% effect at CDMS for $\delta = 100$ keV and a factor of two effect for $\delta = 150$ keV. Because iodine is heavier than germanium, the effect is far milder at DAMA, roughly 10% at $\delta = 150$ keV.

The Earth's speed relative to the galactic rest frame is

$$v_e = v_\odot + v_{orb} \cos\gamma \cos(\omega(t - t_0)). \tag{5}$$

Here $v_\odot = v_0 + 12$ km/s, $v_{orb} = 30$ km/s, $\omega = 2\pi$/year, $t_0 \simeq$ June 2nd, and $\cos\gamma = 0.51$. Defining the dimensionless variables $\eta = v_e / v_0$ and $x_{min} = v_{min}/v_0$, performing the velocity integration in Eq. (2), and applying Eq. (3), one obtains

$$\frac{dR}{dE_R} = \frac{N_T m_N \rho_\chi}{4 v_0 m_\chi} F^2(E_R) \frac{\sigma_n}{\mu_n^2} \frac{(f_p Z + f_n(A-Z))^2}{f_n^2} \times \left(\frac{\mathrm{erf}(x_{min} + \eta) - \mathrm{erf}(x_{min} - \eta)}{\eta}\right). \tag{6}$$

For the DAMA detector, one should take into account there being two species of target nuclei with different quenching factors.

Often one considers the case where $f_n = f_p$ (so that the rate is proportional to A^2), and presents results in the m_χ-σ_n plane. Below we will be particularly interested in models in which the scattering is dominated by vector interactions arising from Z boson exchange, giving $f_n/f_p = -(1 - 4\sin^2\theta_W) \simeq -0.08$ [and yielding a rate that is instead nearly proportional to $(A-Z)^2$]. In all of our calculations we take this value for f_n/f_p.

The differential rate of Eq. (6) depends on the mass splitting parameter δ through x_{min}, which is given by

$$x_{min} = \frac{1}{v_0} \sqrt{\frac{1}{2 m_N E_R}} \left(\frac{m_N E_R}{\mu} + \delta\right), \tag{7}$$

where μ is the reduced mass of the relic-nucleus system. A non-zero δ increases the minimum relic speed required to produce a given nuclear recoil energy. In the following sec-

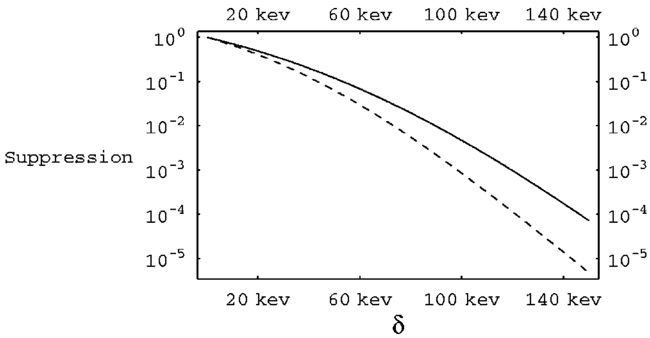

FIG. 1. Ratio of total events in iWIMP scenario to ordinary WIMP as a function of splitting δ for DAMA (solid line) and CDMS (dashed line), with $m_\chi = 50$ GeV. For DAMA we have integrated the total events in the 2–10 keV energy region, while for CDMS we have integrated in the 10–100 keV region. For large δ (>100 keV), the finite value of the the galactic escape velocity can become important, yielding larger suppressions than shown. This effect is stronger for CDMS than for DAMA.

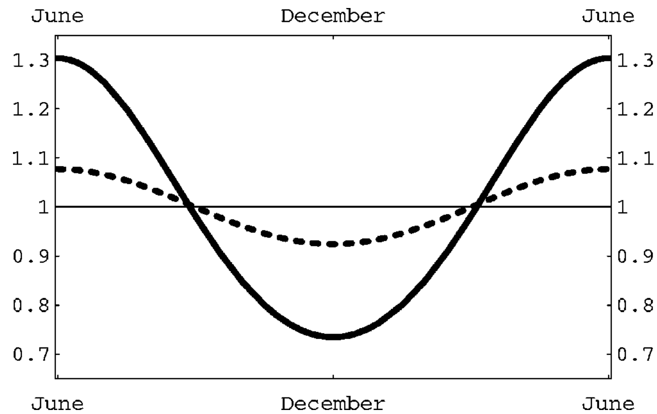

FIG. 2. Annual modulation of event rate with average normalized to one in the inelastic WIMP scenario (solid line) and standard WIMP scenario (dashed line), with $\delta = 100$ keV and $m_\chi = 50$ GeV.

tion we explore potential consequences for direct detection signals arising due to this modification.

III. SIGNALS AT CDMS AND DAMA

Before we study whether there are regions of parameter space that are consistent with both DAMA and CDMS, it is worthwhile to investigate the differences arising when compared with the elastic case. We have seen that for a given velocity of a dark matter particle, it might be that only DAMA is able to detect the particle, and not CDMS. Given the distribution of relic velocities, we can now determine what effect the inelasticity has on the full signal integrated over all velocities. The simplest quantity to consider is the level at which the signal[1] is suppressed when compared with the elastic case. We plot these suppressions for CDMS and DAMA in Fig. 1.

We can easily see that our basic intuition is borne out. The greater the splitting between χ_- and χ_+, the greater the suppression for CDMS compared to that of DAMA. Since the CDMS excluded region only just covers the DAMA preferred region, even a factor of a few can dramatically improve the consistency of the experiments.

However, the relative suppression is not the only relevant quantity because DAMA is not sensitive to the total flux, but rather to the modulation of the flux. Because of the inelasticity, DAMA only sees those particles on the high tail of the Maxwellian distribution. Consequently, a small modulation in the average velocity can lead to much higher modulation for a given signal when compared with the elastic case. This effect is demonstrated in Fig. 2. The combination of these two effects results in DAMA having significant regions of sensitivity that are inaccessible to the existing Ge experiments.

[1]For our purposes here, we will consider the signal to be the events falling in the 10–100 keV bins for CDMS and 2–10 keV for DAMA.

The DAMA signal can be decomposed into background, unmodulated signal and modulated signal as

$$\mu_k = b_k + S_{0,k} + S_{m,k}\cos(\omega t), \tag{8}$$

where k indexes the energy bin of each piece of the total measured events μ. Recently, the DAMA collaboration published its best fit values of $S_{0,k}$ and $S_{m,k}$ for the energy bins 2–3 keV, 3–4 keV, 4–5 keV and 5–6 keV [6]. It is tempting to fit the inelastic scattering case to these values, but to do so would be misleading. These best fit values are derived assuming the energy spectrum and relative size of the modulated piece to be given by the known relations for an elastically scattering WIMP. We have already seen in Fig. 2 that the standard WIMP and inelastic WIMP cases can lead to very different predictions for the relative size of the modulated piece, so any fit to the published best-fit values would not be rigorous.

Another, potentially more significant reason that we cannot use the standard WIMP $S_{m,k}$ values, comes from changes in the energy spectrum of the events. Because the scattering is inelastic, the total number of events may not rise exponentially at low energy. In other cases, the spectra will be nearly identical. As examples we compare in Fig. 3 the expected WIMP spectrum of the modulation signal to the spectrum in the inelastic WIMP scenario for two values of δ. The potential differences revealed in Fig. 3 make it possible to fit only to the model independent data recently published. We will discuss the details of this fit shortly.

These spectrum differences carry over to germanium experiments. As we show in Fig. 4, the changes can again be significant, and can again alter the interpretation of the experimental data. For instance, in the elastic case one expects an exponential rise in the number of relic scattering events for lower energies. Were CDMS to see many events in the 40–60 keV bin, but essentially an absence of events below 40 keV, this would be inconsistent with an elastic dark matter signal, but not with an inelastic dark matter signal. Again, we do not perform a rigorous fit to the CDMS data as this

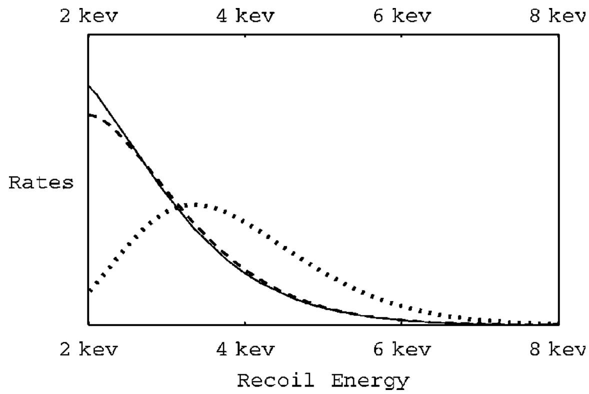

FIG. 3. Normalized modulation (S_m) as a function of energy for ordinary WIMP scenario (solid line), inelastic WIMP scenario with $\delta = 100$ keV (dashed line), and inelastic WIMP scenario with $\delta = 150$ keV (dotted line), all with $m_\chi = 60$ GeV.

would require an ability to accurately simulate the correlation of multiple scatterers with single scatterers, which we lack.

For the purposes of generating allowed regions, we will thus use the following limits: for DAMA, we will use the published model independent modulation in the 2–6 keV bins of 0.088 ± 0.02 counts/day/kg [6] and consider the three sigma region to be allowed. DAMA claims not to have modulation in the higher energy bins. Although the measured modulation for energies above 6 keV is not published, we will take an upper limit of 0.003 counts/day/kg, which we consider quite reasonable given the errors on the best fit values for the higher energy bins. For CDMS, we will require a predicted mean of fewer than six total events, consistent with the published limits [5].

DAMA has also reported null results arising from a pulse shape analysis (PSA) of a portion of their NaI data [13] and of data from an experiment with Xe ($A = 129$) [14]. Using the pulse shape, they can discriminate signal from background, and place a limit on the total number of events. Both of these studies affect the elastic WIMP preferred region for DAMA. Extracting rate limits from tables and plots of [13] and [14], we find the Xe studies have the dominant impact on our allowed regions. For the Xe experiment we require the signal to be less than 0.7 counts/day/kg for the 13–15 keV bin, 0.25 counts/day/kg for the 15–20 keV bin, 0.15 counts/day/kg for the 20–25 keV bin, and 0.075 counts/day/kg for the 25–30 keV bin, consistent with published limits [14].

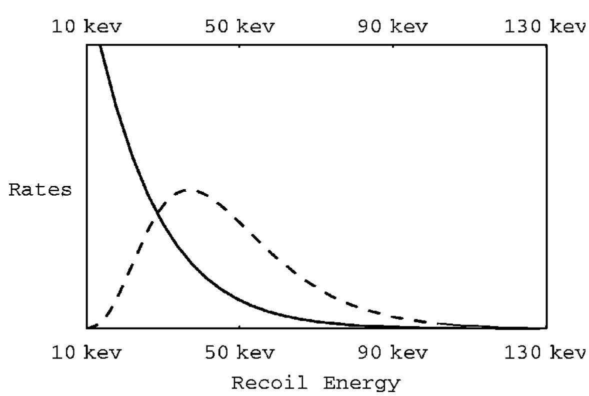

FIG. 4. Normalized spectrum of events at CDMS for ordinary WIMP (solid line) and inelastic WIMP (dashed line) with $\delta = 100$ keV, both with $m_\chi = 50$ GeV.

We show the allowed regions subject to these constraints for various values of m_χ in Fig. 5. As expected, there are broad regions that fit the DAMA data and which are not excluded by CDMS. It is important to note that our qualitative results are not very sensitive to the details of the criteria used to determine what signals are consistent with the experiment. The general features of Fig. 5 remain essentially intact even if we are more conservative in our estimates of the allowed counts at CDMS, or of the accuracy of the measured modulation at DAMA.

As an explicit example, let us consider the point $m_\chi = 70$ GeV, $\delta = 105$ keV and $\sigma_n = 5 \times 10^{-40}$ cm^2. Here the modulation is quite consistent with the DAMA best fit point, but CDMS has only an expected signal of 0.5 events, and the Xe pulse shape analysis constraints are evaded. A comparison between the inelastic point and the DAMA best fit values for the elastic case is given in Table I.

A. Cosmological uncertainties

Unlike the ordinary WIMP scenario, the only inelastic WIMPs that scatter in existing experiments are those on the high end of the Maxwell-Boltzmann velocity distribution. As such, there is greater uncertainty in the precise values of σ_n that fit the data than for an ordinary WIMP.

In particular, there is significant uncertainty in the dispersion velocity v_{rms} and in the local halo velocity v_0. Although these uncertainties are $O(10\%)$, the effects can be amplified because of the presence of the exponential in the distribution. We have investigated these effects and found that the preferred cross sections can shift by as much as a factor of three for $m_\chi = 100$ GeV and a factor of seven for $m_\chi = 50$ GeV. Likewise the local density ρ_χ is uncertain to a factor of approximately two, and moreover, the presence of substructure in the halo of the galaxy can lead to amplifications of the local density relative to the average halo density by a factor of three or more [11].

Finally, we must restate that we have assumed a Maxwell-Boltzmann distribution, which arises in the isothermal sphere model of dark matter. Changes to the velocity profile of the dark matter can have significant effects on the modulation for standard WIMPs [12], and inelastic dark matter potentially is even more sensitive to these changes. Such uncertainties are difficult to quanitify and we do not discuss them further.

Altogether these uncertainties can amount to a change in the preferred σ_n values, but we should emphasize that the sizes of the regions of parameter space that yield consistency between DAMA and CDMS do not change dramatically.

IV. MODELS OF INELASTIC DARK MATTER

Up to this point, we have considered inelastic dark matter as an interesting phenomenological possibility, but have not

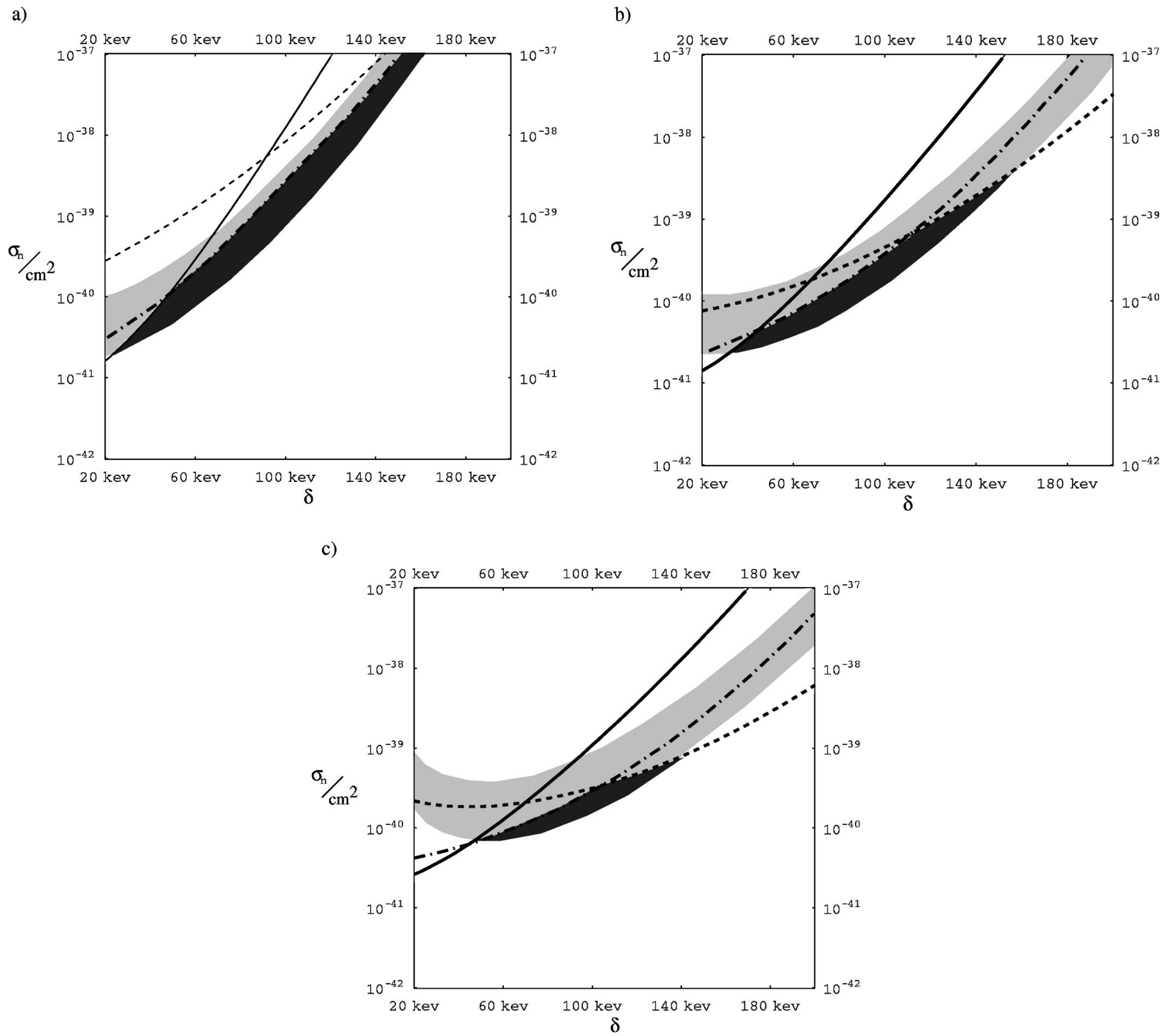

FIG. 5. Regions satisfying both DAMA and CDMS constraints in the $\delta-\sigma_n$ plane, for (a) $m_\chi=50$ GeV, (b) $m_\chi=100$ GeV, (c) $m_\chi=300$ GeV. In each plot, the shaded region has an integrated signal in the $2-6$ keV energy range consistent with the DAMA 3σ region. The solid line gives the CDMS constraint and the dashed line gives the limit from an assumption of the absence of signal in the high energy bins at DAMA. The dot-dashed line gives the upper bound arising from Xe pulse shape analysis limits. The dark shaded region satisfies all constraints simultaneously.

addressed how such particles might arise in a reasonable model. One possibility is that the relic particle is a real scalar, so that its vector coupling to nuclei is forbidden by Bose symmetry. Consider a complex scalar $\phi=(1/\sqrt{2})(a+ib)$ coupled to an Abelian gauge field A_μ. Its vector interaction comes from

$$|D_\mu\phi|^2 \supset -gA_\mu(a\partial^\mu b - b\partial^\mu a). \tag{9}$$

That is, the real scalars a and b couple to each other, but neither couples to itself.

These real scalars are degenerate if the only mass term is $-m^2|\phi|^2$, but introducing a small additional mass term $-\Delta^2\phi^2+\text{H.c.}$ splits this degeneracy.[2] If m is roughly 100 GeV, and we want a splitting ~ 100 keV, then we require $\Delta^2 \sim (100 \text{ MeV})^2$. In the model of Sec. IV A, which features a real component of a sneutrino as the dark matter, this scale for Δ arises naturally.

Before discussing this model, we note that the inelastic dark matter could instead be fermionic. Consider a Dirac fermion $\psi=(\eta\,\overline{\xi})$ that has vector and axial-vector couplings

[2]Of course, Δ violates gauge invariance, and can only arise once the gauge symmetry of the theory has been broken.

TABLE I. Binned signal rates for an inelastic WIMP with $m_\chi = 70$ GeV, $\delta = 105$ keV and $\sigma_n = 5\times10^{-40}$ cm^2, compared with the DAMA best fit values for a standard WIMP. CDMS would have seen an expected 0.5 events.

Energy	iWIMP	DAMA
2–3 keV	0.021	0.023±0.006
3–4 keV	0.014	0.013±0.002
4–5 keV	0.007	0.007±0.001
5–6 keV	0.003	0.003±0.001

to quarks:

$$\bar{\psi}\gamma_\mu(g_V'+g_A'\gamma_5)\psi\bar{q}\gamma^\mu(g_V+g_A\gamma_5)q. \tag{10}$$

Assuming for simplicity that the various g's are of comparable size, the largest contribution to the low-energy scattering of ψ off of nuclei will come from the vector-vector piece, which will yield an amplitude that scales roughly as the number of nucleons. The axial-axial piece yields a smaller spin-dependent contribution that lacks this enhancement, while the vector-axial pieces vanish in the extreme nonrelativistic limit.

Now suppose that in addition to a Dirac mass ~ 100 GeV for ψ, the Lagrangian also contains a very small Majorana mass term $(\delta/2)(\eta\eta+\overline{\eta\eta})$, with $\delta\sim 100$ keV. Then the Majorana fermion mass eigenstates are

$$\chi_1 \simeq \frac{i}{\sqrt{2}}(\eta-\xi) \quad m_1 = m-\delta \tag{11}$$

$$\chi_2 \simeq \frac{1}{\sqrt{2}}(\eta+\xi) \quad m_2 = m+\delta. \tag{12}$$

The vector current essentially couples χ_1 to χ_2, with only a small additional piece $\sim\delta/m$ coupling each mass eigenstate to itself:

$$\bar{\psi}\gamma_\mu\psi \simeq i(\overline{\chi_1}\overline{\sigma}_\mu\chi_2-\overline{\chi_2}\overline{\sigma}_\mu\chi_1)+\frac{\delta}{2m}(\overline{\chi_2}\overline{\sigma}_\mu\chi_2-\overline{\chi_1}\overline{\sigma}_\mu\chi_1). \tag{13}$$

Because $\delta/m\sim10^{-6}$, we ignore the second term, and find that the only way for χ_1 to scatter coherently off of nuclei is to make a transition into the heavier χ_2 state. This inelastic process will dominate relative to the elastic, spin dependent scattering provided that the coherence enhancement, which gives a factor $\sim A^2\sim5\times10^3$ in the cross section, overcomes the suppression due to the inelasticity. In this case, the rate can depend sensitively on the mass of the target nucleus, as desired.

A. Sneutrino dark matter

Interestingly enough, a suitable candidate for inelastic dark matter has already been discussed in the literature. In supersymmetric theories with lepton number violation, the LSP can be a real component of the sneutrino [8,15,16]: a Lagrangian term $-\Delta^2\tilde{\nu}\tilde{\nu}+$H.c. lifts the degeneracy between the sneutrino's odd and even CP eigenstates $\tilde{\nu}_-$ and $\tilde{\nu}_+$. This splitting prevents elastic scattering of the lightest state, $\tilde{\nu}_-$, off of nuclei through Z exchange.[3] There is still the challenge of achieving a cosmologically interesting relic abundance, since an ordinary 100 GeV sneutrino $\Omega_{\tilde{\nu}}$ comes out too small. In [8], this problem was resolved by taking the mass splitting between $\tilde{\nu}_-$ and $\tilde{\nu}_+$ to be large enough to prevent coannihilation via an s-channel Z in the early universe, $\delta>5$ GeV, leading to a radiatively generated neutrino mass $m_\nu>5$ MeV. Different approaches were taken in the models of [15,16,18]. These models feature standard model singlet scalars $\tilde{n}$ that are kept light by a global symmetry [15,16] in analogue to the Giudice-Masiero solution to the μ problem [17], or by a gauged B-L symmetry [18]. The singlet states mix with ordinary sneutrinos through weak scale A terms, so that the gauge interactions of the mass eigenstates are suppressed by mixing angles. This suppression allows for an interesting relic abundance even for values of δ too small to prevent coannihilation between $\tilde{\nu}_-$ and $\tilde{\nu}_+$.

For concreteness we will specialize to the model of [16]. The global symmetry that prevents a tree level mass for the singlet $\tilde{n}$ states is broken by the vacuum expectation valve (VEV) of a spurion X that also breaks supersymmetry. We assume that the A and F components of X both have intermediate scale VEVs: $\langle A_X\rangle\sim\sqrt{\langle F_X\rangle}\sim m_I\sim\sqrt{vM_{Pl}}$. The spurion couples to the neutrino and singlet superfields according to

$$\mathcal{L}\supset\frac{1}{M_{Pl}}[XLNH_u]_F + \frac{1}{M_{Pl}}\left[X^\dagger NN\left(1+\frac{X^\dagger X}{M_{Pl}^2}+\ \ldots\right)\right]_D + \text{H.c.} \tag{14}$$

The operators of Eq. (14) can be justified by ordinary R parity (under which N is odd and X is even), together with an R symmetry where N has R charge 2/3, X has charge 4/3, and L and H_u have R charge 0. As discussed in [16], at tree level Eq. (14) yields a neutrino mass matrix whose light eigenvalue is $\sim v^2/M_{Pl}$. However, Eq. (14) also contains

$$\mathcal{L}\supset -A\tilde{l}\tilde{n}h_u-\Delta^2(\tilde{n}\tilde{n}+\text{H.c.}), \tag{15}$$

with A roughly weak scale and $\Delta^2\sim m_I^5/M_{Pl}^3$. These interactions radiatively induce a Majorana mass for the left-handed neutrino

[3]There are contributions that will induce an elastic scattering, for instance from Higgs exchange, but these are all small and can be ignored for our purposes here.

$$m_\nu \sim \frac{g^2}{384\pi^2}\frac{v^{3/2}}{M_{Pl}^{1/2}} \tag{16}$$

that is larger than that obtained from the tree-level seesaw, and moreover, in roughly the correct range for explaining the atmospheric neutrino anomaly.

For our present purpose, however, the impact of Eq. (15) on the scalar masses is what matters most. Neglecting the small lepton number violating mass parameter Δ, the sneutrino mass-squared matrix is

$$\mathcal{L} \supset -(\tilde{\nu}^* n)\begin{pmatrix} m_L^2 & \frac{1}{\sqrt{2}}Av\sin\beta \\ \frac{1}{\sqrt{2}}Av\sin\beta & m_R^2 \end{pmatrix}\begin{pmatrix}\tilde{\nu} \\ n^*\end{pmatrix}. \tag{17}$$

The A term coupling induces a mixing between $\tilde{\nu}$ and $\tilde{n}$, yielding a lighter mass eigenstate

$$\tilde{\nu}_1 = -\tilde{\nu}\sin\theta + \tilde{n}^*\cos\theta. \tag{18}$$

The coupling of $\tilde{\nu}_1$ to the Z boson is thus suppressed by $\sin^2\theta$. The lepton number violating parameter Δ^2 lifts the degeneracy between the CP-even and CP-odd components of $\tilde{\nu}_1$, leading to a small mass difference

$$\delta \simeq 2\cos^2\theta\frac{\Delta^2}{m_1}. \tag{19}$$

For this splitting to resolve the conflict between CDMS and DAMA, one needs $\delta \sim 50-100$ keV, roughly.[4] For a 100 GeV sneutrino, this implies $[X^\dagger X X^\dagger]_D \sim m_I^5 \sim (3\times 10^{10}\ \text{GeV})^5$, corresponding to a reasonable value for the intermediate scale.

To explore the feasibility of this scenario, we apply the same criteria used in Sec. III to establish consistency with CDMS and DAMA for $\delta = 50$ and 100 keV, and display the allowed regions in the $(m_{\tilde{\nu}}, \sin\theta)$ plane. Note that because the scattering off of nuclei is suppressed both by the inelasticity of the reaction and by a $\sin^4\theta$ factor, the ability to obtain a large enough signal at DAMA depends crucially on the fact that ordinary sneutrinos give a signal roughly three orders of magnitude above present bounds. We also calculate the relic abundance as a function of $m_{\tilde{\nu}}$ and $\sin\theta$ using standard methods. The results shown in Figs. 6(a)–6(d) indicate that there are indeed regions of parameter space featuring interesting relic abundances and acceptable direct detection rates. In the early universe, the efficiency of annihilation processes that occur via s-channel Higgs exchange, such as $\tilde{\nu}_-\tilde{\nu}_- \to b\bar{b}$, ZZ, W^+W^-, are sensitive to the size of the trilinear scalar coupling A, leading to the dependence of the relic abundance on A evident in the figures.

Just as one specific illustrative example, consider the parameters $m_{\tilde{\nu}} = 70$ GeV, $\delta = 70$ keV, and $\sin^4\theta = 1/70$. This choice of $\sin\theta$ leads to an interesting relic abundance for a broad range of SUSY parameters. For this choice of $m_{\tilde{\nu}}$, δ, and $\sin\theta$, we calculate a mean of less than 2 events at CDMS and satisfy the constraints from the Xe pulse shape analysis. Moreover, as shown in Table II, the values of $S_{m,k}$ we obtain for DAMA in the 2–6 keV energy range are nearly identical to those we obtain in the elastic case using DAMA's best fit point $\sigma_n = 7.2\times 10^{-6}$ pb and $m_\chi = 52$ GeV.

B. Indirect detection

As dark matter passes through the Sun, it can scatter off of nuclei and be captured in the Sun's potential well [19]. After a significant amount of dark matter has been captured, it can annihilate into other particles. If muon neutrinos are produced, those that reach the Earth can produce high energy muons through charged-current interactions. A number of experiments have attempted to detect WIMP matter indirectly by looking for these upward-going muons, leading to a current limit on their flux of $10^{-14}\ \text{cm}^{-2}\ \text{s}^{-1}$ [20–22].

Even within the model of Sec. IV A, the expected flux of upward-going muons is quite uncertain, for a number of reasons. First, the capture rate in the Sun is sensitive to the parameters $m_{\tilde{\nu}}$, $\sin\theta$ and δ. Second, if the captured sneutrinos annihilate directly into neutrinos, the flavor of the lightest sneutrino determines what flavor of neutrino is produced, and details of the neutrino masses and mixings impact the flavor of the neutrino detected at the Earth. Third, cosmological uncertainties mentioned in Sec. III A can change the preferred region of σ_n and thus the capture rate. Finally, relatively minor extensions to the model of Sec. IV A can also complicate matters. As a consequence of these various sources of uncertainty, indirect techniques do not rule out inelastic sneutrino dark matter. However, they do impose strong constraints, as broad regions of parameter space lead to signals above experimental bounds. Moreover, indirect detection experiments offer the strong possibility of detection if the bound on the muon flux improves considerably [23].

One might expect that the same inelasticity that suppresses the signal at CDMS should be even more effective in suppressing the capture rate by the Sun, which is mainly composed of relatively light nuclei. In fact, this is typically not the case. Because particles passing through the Sun are unusually energetic (the escape velocity at the surface of the Sun is much larger than the average velocity of a halo particle), the inelasticity is *less* relevant in the Sun than at direct detection experiments.

In what follows, we have followed [24] in calculating solar capture rates and the induced muon flux, but have modified the approach to approximate the suppression of the capture rate due to the inelasticity (see Appendix). This sup-

[4]The lifetime of $\tilde{\nu}_+$ is $\tau \simeq ((1/3)/\sin\theta)^4(100\ \text{keV}/\delta)^5(4\times 10^2\ \text{yr})$, so for the mass splittings and mixing angles of interest, it is safe to assume that only $\tilde{\nu}_-$ is present today. Photons can be produced in these decays, but the decays take place before recombination for the parameters of interest, and the photons are soft enough to render negligible the effect on the cosmic microwave background radiation (CMBR) spectrum.

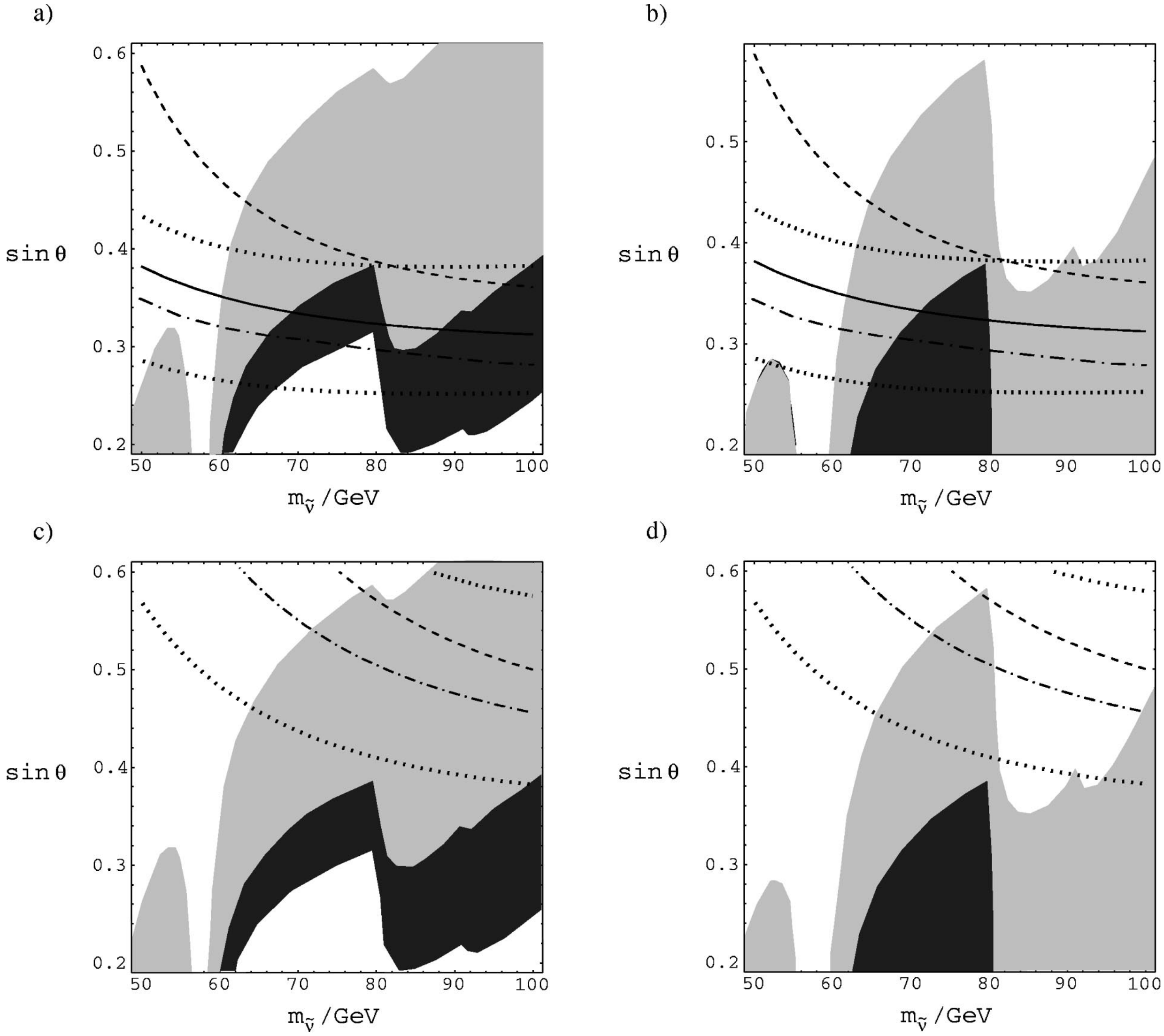

FIG. 6. For the sneutrino dark matter case, regions that satisfy the direct detection requirements of Sec. III, plotted along with filled contours of $\Omega_{\tilde{\nu}}h^2$. The lighter shaded region corresponds to $0.05<\Omega_{\tilde{\nu}}h^2<0.3$ and the darker shaded region corresponds to $0.3<\Omega_{\tilde{\nu}}h^2<0.64$. The region between the dotted contours has an integrated signal in the 2–6 keV range consistent with the DAMA 3σ region. The solid line gives the CDMS constraint, the dashed line gives the limit from the absence of signal in the high energy bins at DAMA, and the dot-dashed line gives the constraint arising from Xe pulse shape analysis data (regions below these lines are allowed). We take $\delta=50$ keV for (a) and (b) and $\delta=100$ keV for (c) and (d). For (a) and (c), we use $A=25$ GeV, while for (b) and (d), we take $A=50$ GeV. For each plot we take $\tan\beta=50$, $m_h=115$ GeV, and a bino mass of 300 GeV, with the assumption of grand unified theory (GUT) unification of gaugino masses.

TABLE II. $S_{m,k}$ values obtained using DAMA's best fit point, $\sigma=7.2\times10^{-6}$ pb and $m_\chi=52$ GeV for the standard WIMP case, and values obtained taking $\delta=70$ keV, $m_{\tilde{\nu}}=70$ GeV, and $\sin^4\theta=1/70$ for the sneutrino inelastic dark matter case.

Energy/keV	$S_{m,k}$(cpd/kg/keV)	
	DAMA best	inelastic $\tilde{\nu}$
2–3	0.027	0.027
3–4	0.013	0.013
4–5	0.005	0.006
5–6	0.002	0.002

pression depends on the mass of the nucleus. For example, for $\delta=100$ keV and $m_{\tilde{\nu}}=100$ GeV, we find a factor ~ 20 suppression for scattering off of oxygen in the Sun, and a factor ~ 2 suppression for scattering off of iron.

We will separately consider first the case in which the sneutrinos cannot annihilate into W's, and second, the case in which they can. For $m_{\tilde{\nu}}<m_W$, sneutrinos in the Sun typically annihilate dominantly to neutrinos via t-channel neutralino exchange. If we neglect cosmological uncertainties, we find that for values of $m_{\tilde{\nu}}$, δ and $\sin\theta$ that lead to interesting relic abundances and consistency with CDMS and DAMA, the flux of neutrinos produced is quite large. If these are all muon flavor, we would expect a flux of upward-going muons of at least $\sim 6\times10^{-13}$ cm^{-1}s^{-1}, in conflict with ex-

perimental results. On the other hand, if the sneutrinos annihilate into electron neutrinos that do not oscillate into muon neutrinos, bounds from direct detection are evaded entirely. If this is the case, only direct detection experiments will be able to yield a positive signal.

Finally, we note that there are specific parameter choices for which the dominant annihilation of sneutrinos in the Sun is through *s*-channel Higgs to $b\bar{b}$. We find that this allows the flux of upward-going muons to be as small as a factor of ~ 2 above current limits for parameters that yield an acceptable abundance and acceptable direct detection signals.

With cosmological uncertainties included, more scenarios are allowed. Relatively small variations in v_{rms} can accommodate factors of two, such as if the dominant annihilation is into $b\bar{b}$. Direct annihilation into muon neutrinos would require a more specious conspiracy of errors. For instance, if the solar system were presently in an anomalously high density region of the galaxy arising from substructure, and if v_{rms} were 3σ above the value we have used, experiments could accomodate as much as one-third of the neutrinos produced being muon flavored. This seems quite unlikely, but is, at least in principle, still allowed.

However, for these lighter sneutrinos, if indirect detection experiments improve by an order of magnitude, they will be able to probe almost all of the parameter space, even accounting for a broad class of cosmological uncertainties, and situations where there is annihilation to $b\bar{b}$.

For heavier sneutrinos ($m_{\tilde{\nu}} > m_W$), the dominant annihilation processes in the Sun can easily be *s*-channel Higgs exchange to *W*'s and *Z*'s. In this case we find that it is possible to reduce the expected signal at direct-detection experiments to a factor of ~ 3 above current limits for parameters consistent with DAMA, CDMS, and $\Omega_{\tilde{\nu}} h^2 \sim 0.1$. These heavier sneutrinos are less affected by cosmological uncertainties, but these uncertainties still make it impossible to rule out this scenario. Future improvements in indirect detection could rule out this region of parameter space, especially as the experimental signal is less sensitive to the flavor of the lightest sneutrino than for the case of $m_{\tilde{\nu}} < m_W$.

Of course, this discussion applies only to the model of Sec. IV A, and one can consider modifications to the model that suppress the indirect detection signal. The premise of the model is that light standard model singlets are natural. Given this, if we add to that model another standard model singlet η, with the same *R*-charge as the right-handed neutrino *N*, but opposite *R*-parity, we expect a superpotential interaction ηNN. Then through *t*-channel η exchange, $\tilde{\nu}$'s can annihilate to right-handed neutrinos. If these decay dominantly into muons or electrons (rather than tau's) and off-shell *W*'s, we find that it is possible to bring the flux of upward going muons induced by the *W* decay products down to current limits.[5] Future indirect experiments would still likely be able to see the decay products of these right-handed neutrinos.

This is just one example of a modification to the model which diminishes the signal, and there may be others, but such uncertainty is difficult to quantify. While indirect experiments offer a good opportunity to test specific models and regions of parameter space, there is an excellent likelihood that upcoming direct detection experiments will be able to determine whether inelastic dark matter is the resolution of the conflict between DAMA and CDMS.

V. FUTURE EXPERIMENTS

In the inelastic dark matter scenario, the boundaries of the DAMA preferred region are not far from the current limits from CDMS. Planned experiments should be able to cover the existing DAMA region. Most important are planned improvements to germanium experiments, and the CRESST experiment, which will use the heavy element tungsten.

CDMS will soon be moving to the Soudan mine, and should be able to improve its limits by at least two orders of magnitude [25]. The GENIUS Ge experiment [26] should go well below that, likely allowing both to test much of the preferred regions discussed in Sec. III.

There is a caveat in this statement: in generating the plots of Fig. 5, we neglected to include the effect of a finite galactic escape velocity. This was a harmless simplification for our purposes there, because the effects at DAMA due to the finite galactic escape velocity are relatively minor. The effects can be much larger at CDMS.

Recall that the requirement for scattering is

$$\delta < \frac{\beta^2}{2} \frac{m_N m_\chi}{m_N + m_\chi}. \tag{20}$$

This constraint is particularly stringent for light candidates. For instance, with $m_\chi = 50$ GeV and $v_{esc} = 650$ km/s, Eq. (20) tells us that only for $\delta < 122$ keV can one hope to obtain any signal at all at a germanium detector (recall that the highest velocity of particles incident on the Earth is $v_{esc} + v_\odot$). Thus, the higher δ regions may not be testable at CDMS.

For heavier candidates, the finite galactic escape velocity is not especially important, even at CDMS. With a galactic escape velocity of 650 km/s, and $m_\chi = 100$ GeV, the cutoff for δ is 172 keV. On the other hand, the galactic escape velocity is not a particularly well known quantity, and if instead we take $v_{esc} = 450$ km/s, the cutoff for δ is only 102 keV.

These uncertainties make the CRESST experiment [27], using tungsten, especially significant. Because tungsten ($A = 183$) is heavier than iodine ($A = 127$), given adequate exposure time, CRESST should cover the DAMA preferred region, irrespective of cosmological uncertainties.

A very real possibility is that both germanium and tungsten experiments *will* have signals, which, when interepreted as elastic scatterings, would be inconsistent with one another. The most striking possibility of all is a spectrum deformation at the germanium detectors, as discussed in Sec. III. If CDMS were to see an excess of events in the 30

---

[5] In such a scenario, the relic abundance is modified, but it is still possible to have $\Omega_{\tilde{\nu}} h^2 \sim 0.1$.

-70 keV region, but no excess below 30 keV, it would be a compelling signature of this scenario.

VI. CONCLUSIONS

If in fact the majority of the matter of the universe is nonbaryonic, the attempt to determine its nature is one of the most exciting endeavors of modern cosmology. Existing dark matter searches have already begun to probe interesting regions of parameter space for candidate particles such as neutralinos and axions.

The positive result from the DAMA experiment is difficult to understand in terms of these candidates, as it is in seeming conflict with constraints arising from the CDMS experiment. We have seen that this conflict vanishes if we allow for the possibility that the dark matter particle can only scatter inelastically.

We have shown that the sneutrino, when mixed with a singlet scalar with weak lepton number violation, is a viable candidate for inelastic dark matter. The regions of parameter space which give an interesting relic sneutrino abundance overlap with the regions which give a positive DAMA signal. Indirect detection experiments tightly constrain models of sneutrino dark matter, but do not rule them out.

Even absent a particular model, we find it interesting that such a simple modification of the dark matter's properties can give remarkably different predictions, including the suppression of a signal at CDMS. We consider these results sufficiently interesting as to warrant an analysis of the full DAMA data set should the raw data become available.

ACKNOWLEDGMENTS

We thank L. Hall, W. Haxton, C. Hogan, L. Wells, and T. Quinn for useful discussions, and H. Murayama and A. Nelson for reading the paper and providing valuable comments. This work was supported in part by the U.S. Department of Energy under Contracts DE-AC03-76SF00098, in part by the National Science Foundation under grant PHY-95-14797.

APPENDIX

Here we describe how we approximate the suppression of the rate of relic capture by the Sun due to the inelasticity of the scattering. Ignoring nuclear form factors, the scattering probability for a given relative velocity w is equally distributed between the minimum and maximum nuclear recoil energies ΔE_{min} and ΔE_{max} (these parameters depend on the nucleus mass, the relic mass m, w, and δ). Ordinarily, the low-energy scattering cross section is independent of w, but in the inelastic case there is an additional phase space factor $\sqrt{1-2\delta/(\mu w^2)}$, where μ is the reduced mass. Capture only occurs when $\Delta E > \Delta E_{capture} \equiv 1/2(mw^2-(m+\delta)v_{esc}^2(r)) - \delta$ holds. Here $v_{esc}(r)$ is the (position-dependent) escape velocity, which we approximate as [24]

$$v_{esc}(r) = v_c^2 - \frac{M(r)}{M_\odot}(v_c^2 - v_s^2), \tag{A1}$$

where $v_c = 1354$ km/s, $v_s = 795$ km/s, and $M(r)$ is the mass contained within the radius r. The capture rate off of a given species of nuclei is then proportional to

$$\int_0^{R_\odot} dr\, r^2 \rho(r) \int_{v_{esc}}^{\infty} dw\, w^3 e^{-\frac{(w^2-v_{esc}^2)}{v_0^2}} \sqrt{1-2\delta/(\mu w^2)} \times \left(\frac{\Delta E_{max} - \Delta E_{capture}}{\Delta E_{max} - \Delta E_{min}} \right), \tag{A2}$$

where $\rho(r)$ is the mass density of the species and v_0 is the rotational speed of the local standard of rest. We calculate this factor (which does not account for form factor suppressions) in the elastic ($\delta = 0$) and inelastic cases to estimate the suppression coming from the inelasticity. We then obtain capture rates by multiplying this suppression with the rate obtained for the elastic case using the formulas of [24] (which do include form factor suppressions).

[1] V. Trimble, Annu. Rev. Astron. Astrophys. **25**, 425 (1987).

[2] MACHO Collaboration, C. Alcock *et al.*, Astrophys. J. **542**, 281 (2000).

[3] B. W. Lee and S. Weinberg, Phys. Rev. Lett. **39**, 165 (1977).

[4] L. Baudis, A. Dietz, B. Majorovits, F. Schwamm, H. Strecker, and H. V. Klapdor-Kleingrothaus, Phys. Rev. D **63**, 022001 (2001).

[5] CDMS Collaboration, R. Abusaidi *et al.*, Nucl. Instrum. Methods Phys. Res. A **444**, 345 (2000).

[6] DAMA Collaboration, R. Bernabei *et al.*, Phys. Lett. B **480**, 23 (2000).

[7] P. Ullio, M. Kamionkowski, and P. Vogel, hep-ph/0010036.

[8] L. J. Hall, T. Moroi, and H. Murayama, Phys. Lett. B **424**, 305 (1998).

[9] K. Freese, J. A. Frieman, and A. Gould, Phys. Rev. D **37**, 3388 (1988).

[10] R. H. Helm, Phys. Rev. **104**, 1466 (1956); J. Engel, Phys. Lett. B **264**, 114 (1991).

[11] B. Moore, S. Ghigna, F. Governato, G. Lake, T. Quinn, J. Stadel, and P. Tozzi, astro-ph/9907411.

[12] J. D. Vergados, Phys. Rev. D **62**, 023519 (2000).

[13] R. Bernabei *et al.*, Phys. Lett. B **389**, 757 (1996).

[14] R. Bernabei *et al.*, Phys. Lett. B **436**, 379 (1998).

[15] N. Arkani-Hamed, L. Hall, H. Murayama, D. Smith, and N. Weiner, hep-ph/0006312.

[16] N. Arkani-Hamed, L. Hall, H. Murayama, D. Smith, and N. Weiner, hep-ph/0007001.

[17] G. F. Giudice and A. Masiero, Phys. Lett. B **206**, 480 (1988).

[18] F. Borzumati and Y. Nomura, hep-ph/0007018.

[19] J. Silk, K. Olive, and M. Srednicki, Phys. Rev. Lett. **55**, 257 (1985); L. M. Krauss, K. Freese, D. N. Spergel, and W. H. Press, Astrophys. J. **299**, 1001 (1985).

[20] Super-Kamiokande Collaboration, A. Okada, astro-ph/0007003.

[21] MACRO Collaboration, D. G. Michael, 29th International Conference on High-Energy Physics (ICHEP 98), Vancouver, British Columbia, Canada, 1998.

[22] J. M. LoSecco *et al.*, Phys. Lett. B **188**, 388 (1987).

[23] AMANDA Collaboration, F. Halzen *et al.*, Prepared for 26th International Cosmic Ray Conference (ICRC 99), Salt Lake City, Utah, 1999.

[24] A. Gould, Astrophys. J. **388**, 338 (1992); G. Jungman, M. Kamionkowski, and K. Griest, Phys. Rep. **267**, 195 (1996).

[25] B. Sadoulet, in *Proceedings of the 19th International Symposium on Photon and Lepton Interactions at High Energy LP99*, edited by J. A. Jaros and M. E. Peskin [eConf **C990809**, 687 (2000)].

[26] GENIUS Collaboration, H. V. Klapdor-Kleingrothaus *et al.*, hep-ph/9910205.

[27] P. Di Stefano *et al.*, hep-ex/0011064.